Hydrogeophysical monitoring of intense rainfall infiltration in the karst critical zone: A unique electrical resistivity tomography data set

Simon D Carrière, Konstantinos Chalikakis

Data in Brief 40 (2022) 107762

Contents lists available at ScienceDirect

Data in Brief

journal homepage: www.elsevier.com/locate/dib

Data Article

Hydrogeophysical monitoring of intense rainfall infiltration in the karst critical zone: A unique electrical resistivity tomography data set

Simon D. Carrière[a,*], Konstantinos Chalikakis[b]

[a] Sorbonne Université, UMR 7619 METIS (UPMC/CNRS/EPHE), 4 place Jussieu, Paris 75005, France
[b] Avignon Université, UMR 1114 EMMAH (AU/INRAE), 301 rue Baruch de Spinoza, BP 21239 84911, Avignon Cedex 9, France

ARTICLE INFO

Article history:
Received 15 October 2021
Revised 22 December 2021
Accepted 23 December 2021
Available online 25 December 2021

Keywords:
Hydrogeophysics
Recharge monitoring
Critical zone
Karst
Mediterranean

ABSTRACT

The common hydrogeological concepts assume that water mostly enters and flows in fractured and karstified media through preferential pathways related to discontinuities. But it is difficult to locate discontinuities and even more to relate those to possible or effective water routes, particularly when soil or scree covers near surface features. When and where does water flow underground? How fast? Are we able to monitor the infiltration processes? A unique large scale Electrical Resistivity Tomography (ERT) surface based time-lapse experiment was carried out in fractured and karstified carbonate rock during a typical Mediterranean autumn rainy episode (230mm of rain over 17 days). 120 ERT time-lapse sections were measured over the same profile during and after this event (30 days). The gradient array was chosen for his robustness and rapidity. The site is covered by typical Mediterranean forest and is a good example of the surface conditions found in Mediterranean karst. There is no major karstification features (i.e. cave, sinkhole) or major tectonic accident (i.e. fault). In a previous paper, several commercial and research inversion software were tested on this dataset. This processing highlighted some limitations in in-

DOI of original article: 10.1016/j.scitotenv.2019.134247
* Corresponding author.
E-mail address: simon.carriere@upmc.fr (S.D. Carrière).

https://doi.org/10.1016/j.dib.2021.107762

version process. At the actual stage, apparent resistivity data provides insight about recharge/discharge processes that are almost valuable as the inverted resistivity results. Due to his quality, the availability of this unique dataset acquired under natural conditions will allow to the scientific and engineer community exploring advances and limits of ERT approach and to test new software or new data processing strategy.

Specifications Table

Subject	Geophysics
Specific subject area	Karst recharge monitoring using hydrogeophysics
Type of data	Table Figure
How data were acquired	An electrical resistivity tomography (ERT) cross-section was installed perpendicular to the slope. The acquisition was performed with an ABEM TERRAMETER SAS4000 and 64 electrodes two meters spaced. The gradient array was chosen for his robustness and rapidity. This protocol totals 1360 measurement points with a maximum "na" spacing of 80m and the maximum "sa" spacing of 96 m.
Data format	Raw data
Parameters for data collection	For each measurement point, the acquisition time was 0.1 s and the delay time was 0.2 s. Each measurement point cycle spend around 1.8 s. To ensure data quality, during acquisition if a data point presented a repetition Root Mean Square (RMS)>1%, the measurement was repeated until five times (5 stacks). The injection intensity ranges between 50 and 200 mA according to ground resistance.
Description of data collection	The device was installed before the rain and the acquisition was repeated 106 times with a time step ranging from 3 h to a few days. Before the rain, the time step was about 1 day. During the rain the time step was reduced to 3 h during the heaviest rainfall. After the rain the time step was progressively increased until a few days.
Data source location	Institution: LSBB laboratory (http://lsbb.eu/presentation/) City/Town/Region: Rustrel Country: France Latitude and longitude: 43°56'12.15"N; 5°27'58.18"E; 530 m.a.s.l.
Data accessibility	1/ Raw data: Repository name: Mendeley Direct URL to data: http://dx.doi.org/10.17632/vyzmvnj8hr.1 2/ Secondary Data (.DAT): Repository name: Hplus data base Direct URL to data: hplus.ore.fr/public/requests/lsbb/LSBB_ERT_data_Carriere_24102011.csv.tgz
Related research article	[1] S.D. Carrière, K. Chalikakis, C. Danquigny, R. Clément, C. Emblanch, Feasibility and Limits of Electrical Resistivity Tomography to Monitor Water Infiltration Through Karst Medium During a Rainy Event, in: B. Andreo, F. Carrasco, J.J. Durán, P. Jiménez, J.W. LaMoreaux (Eds.), Hydrogeological and Environmental Investigations in Karst Systems, Springer Berlin Heidelberg, 2015: pp. 45–55. https://doi.org/10.1007/978-3-642-17435-3_6.

Value of the Data

- Unique monitoring of intense rainfall infiltration in karst critical zone under natural conditions.
- This dataset will be useful for geophysicists or hydrologists interested in water transfers in the critical zone
- Clean and reusable dataset to improve time-lapse ERT post-processing analysis.
- High quality ERT monitoring repeated 120 times.

1. Data Description

Table 1 presents the first 10 rows and columns of the database including raw data. Column 1 presents the distance along the ERT profile. Column 2 represents the pseudo-depth calculated for a gradient array using the formula developed by Dahlin and Zhou [2]. The 106 following columns present the apparent resistivity for each time steps (after filtering). There are 1360 values of apparent resistivity for each time step.

2. Experimental Design, Materials and Methods

2.1. Study site

The study site is located in the Rustrel Forest in southern France (05° 27′ 57.9′′ E, 43° 56′ 12.2′′ N and elevation 520 m; Fig. 1a) and within the Fontaine-de-Vaucluse hydrosystem (Fig. 2b) which is part of OZCAR (http://www.ozcar-ri.org/), the French network of critical zone observatories.

The study site is located above LSBB laboratory (http://www.lsbb.eu), a tunnel dug for a military purpose and converted into a research laboratory in 1997. The tunnel is located 33 m under the study site and intersect arbitrarily the karst medium. At the surface, the site is covered by typical Mediterranean forest and is a good example of the surface conditions found in the Fontaine-de-Vaucluse hydrosystem. There is no major karstification features (i.e. cave, sinkhole) or major tectonic accident (i.e. fault).

The underground (soil and subsoil) is highly complex; the medium is heterogeneous due to numerous vertical fractures and karstified carbonate rock. Geophysical prospection showed that north-south oriented faults impose the general spatial structure on geology and pedology.

2.2. Climate

The climate is Mediterranean, characterized by cool dry winters, hot and dry summers, and a high inter-annual variability. Most of the rainfall occurs in spring (March to June) and autumn (September to December). Between 1970 and 2018, annual rainfalls ranged from 407 to 1405 mm with a mean of 909 mm. This unique large scale ERT surface based experiment was carried out during a typical Mediterranean autumn rainy episode (17 days). A total of 230 mm of rain was registered and 120 ERT time-lapse sections were measured over the same profile during and after the event (30 days).

2.3. Implantation/acquisition strategy and field constraints

The chosen ERT profile follows an East/West direction. This direction is perpendicular to the general slope, it is sub-perpendicular to one of the main faulting and lineament directions and it

Table 1
First ten columns and rows of the database compiling ERT monitoring raw data.

Distance (m)	Date hour Pseudo-depth/ Altitude (m)	24/10/11 21h Apparent Resistivity (ohm.m)	25/10/11 00h Apparent Resistivity (ohm.m)	25/10/11 03h Apparent Resistivity (ohm.m)	25/10/11 06h Apparent Resistivity (ohm.m)	25/10/11 09h Apparent Resistivity (ohm.m)	25/10/11 12h Apparent Resistivity (ohm.m)	25/10/11 15h Apparent Resistivity (ohm.m)	25/10/11 18h Apparent Resistivity (ohm.m)
3	528.8	1804.81	1812.13	1860.31	1350.34	1291.00	1273.42	1166.19	1157.35
6	527.8	1888.15	1904.56	1971.55	1515.29	1464.01	1443.49	1336.81	1328.25
5	528.1	1888.54	1900.09	1840.60	1332.47	1294.70	1275.61	1200.26	1196.02
9	526.7	1670.44	1687.38	1905.80	1755.66	1719.67	1715.22	1600.32	1593.95
12	525.7	1450.81	1456.72	1568.59	1542.23	1537.35	1549.01	1497.47	1499.27
10	526.4	1342.44	1352.30	1504.44	1514.97	1519.92	1535.36	1491.50	1494.76
15	524.7	1604.84	1605.46	1666.57	1660.36	1656.07	1664.22	1627.63	1629.08

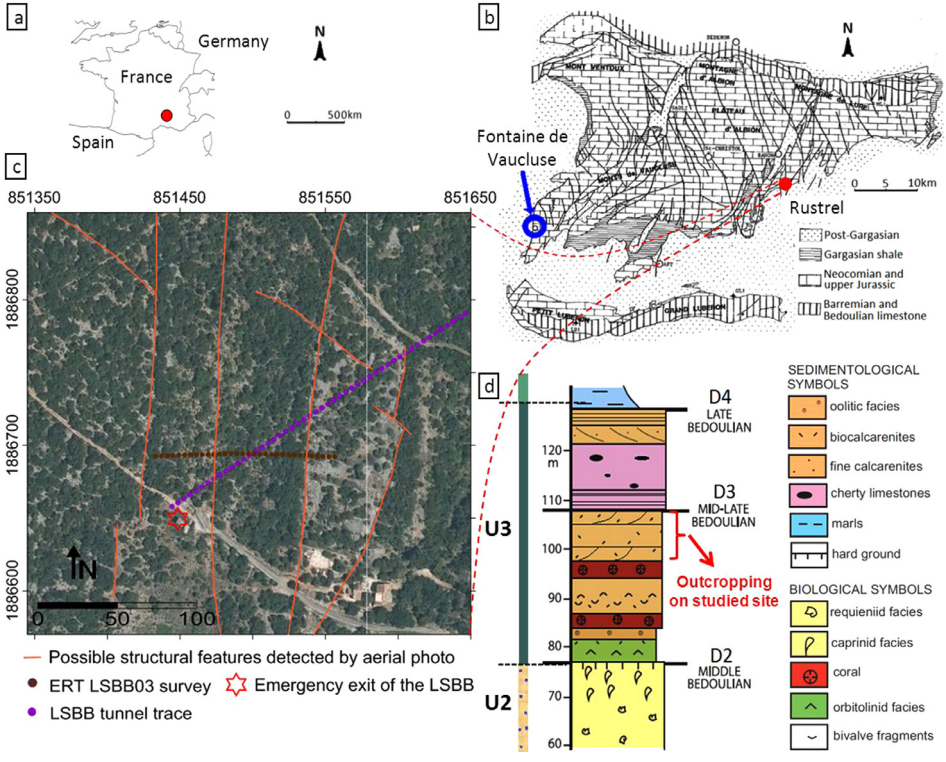

Fig. 1. (a) Fontaine-de-Vaucluse basin located in France; (b) Test site located in Fontaine-de-Vaucluse basin [4]; (c) Aerial photo with main lineament detection and survey location (www.geoportail.gouv.fr); (d) Regional lithostratigraphic log ([5] modified).

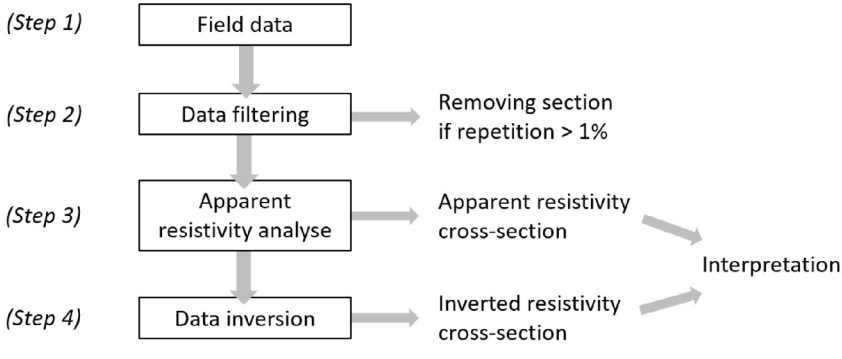

Fig. 2. Data management and processing chain.

is the most heterogeneous direction, in term of apparent resistivity spatial distribution (Fig. 1c). The acquisition system used for ERT time-lapse measurements is an ABEM Terrameter SAS 4000 [3] with 4 channels and 64 electrodes. The profile has 126 m length and a 2 m inter-electrode spacing. Satisfactory contact resistance were obtained around 3 kΩ for few electrodes before the rain. A special attention was given to maintain good contact because bad electrode-ground contact could induce artifacts during data acquisition. For the time-lapse measurements the gradient array was chosen for his robustness and rapidity [2]. This protocol totals 1360 measurement

points with a maximum "na" spacing of 80m and the maximum "sa" spacing of 96 m. For each measurement point, the acquisition time was 0.1 s and the delay time was 0.2 s. Each measurement point cycle spend around 1.8 s. To ensure data quality, during acquisition if a data point presented a repetition Root Mean Square (RMS)>1%, the measurement was repeated until five times (5 stacks). The injection intensity ranges between 50 and 200 mA according to ground resistance. A 50 Hz filter was also applied to reduce anthropogenic noise. During the 30 days campaign, ERT time-lapse acquisition ranges between every three hours during the rainy event (17 days) until one section a day after the rainy event.

2.4. Data management and apparent resistivity visualization

The field data interpretation requires several steps as shown in Fig. 2.

Step 1: The dataset totals of 120 ERT cross-sections. A quality check is required.

Step 2: The data cleaning step is required to remove incorrect or irrelevant data within the dataset. When at least a repetition measurement RMS of one point within the section is superior to 1%, the data acquisition quality was considered not satisfactory. Poor quality data or gaps in the data sets can lead to misinterpretation. The removed 14 ERT cross-sections were acquired before the rain event. This decreased data quality was due to the dryness of the soil that declined the contact between soil and electrodes. To ensure good quality data before the rain, it was necessary to add salty mud on some electrodes. This common practice improved the soil/electrode contact. After data cleaning, a total of 106 ERT sections were kept to follow data treatment.

Step 3: The visualization of apparent resistivities allows to evaluate the consistency of the data regarding the rainfall event (Fig. 3). It is the first interpretation step. Apparent resistivity values have been arithmetically averaged for each section to represents the Fig. 3b. This mean apparent resistivity decreased strongly during the rain event, from 1750 to 1050 Ω.m. These variations do not seem related with temperature variations because air and groundwater temperature remained stable during the campaign [6]. Thus, it can reasonably relate these resistivity variations with water content variation. Analysis of this mean apparent resistivity indicator allows selecting twelve critical times step presented in Fig. 3a, before, during and after the rainy event.

During ERT surveys apparent (measured) resistivity (ρ_α) analysis is usually neglected. However, this rough data could provide, without calculation artifacts, complementary information to the inverted resistivity. In order to visualize data (Fig. 3a), hourly apparent resistivity variations ($\Delta\rho_a$) were calculated between two consecutive time steps. These variations are normalized by the time (Δ_T) between both measurement (ρ_n and ρ_{n-1}) using the following equation (Eq. (1)).

$$\Delta\rho_\alpha = \left(\frac{\rho_{n-1}}{\rho_n} - 1\right) * \frac{100}{\Delta_T} \tag{1}$$

Thus, the data is presented (Fig. 3a) in hourly percentage change in ρ_α with a simplified representation of vegetation and soil cover of the profile. Previously recognized karst features are also presented [7].

At the beginning of the rainy event (Fig. 3a / Section 1→2), ρ_α decrease moderately and homogeneously along the section. This resistivity decrease could be related with a moistening of the near surface horizons. After the first rainy event (Fig. 3a / Section 2→3), ρ_α is early stabilized.

During the following strong rainy episode (Fig. 3a / Sections 4→5 to 7→8), moistening process appears very heterogeneous and some zones look like preferential water pathways (distance -60 m, 0 m, 40 m). These observed variations can be directly influenced by near surface variations. Just after the rain (Fig. 3a / Sections 9→10 and 10→11), ρ_α increases in some zones. That could be related with drainage process because water loss from soil will cause an increase in resistivity due to loose in electrolytic conductivity. These zones are well fitted with some zones

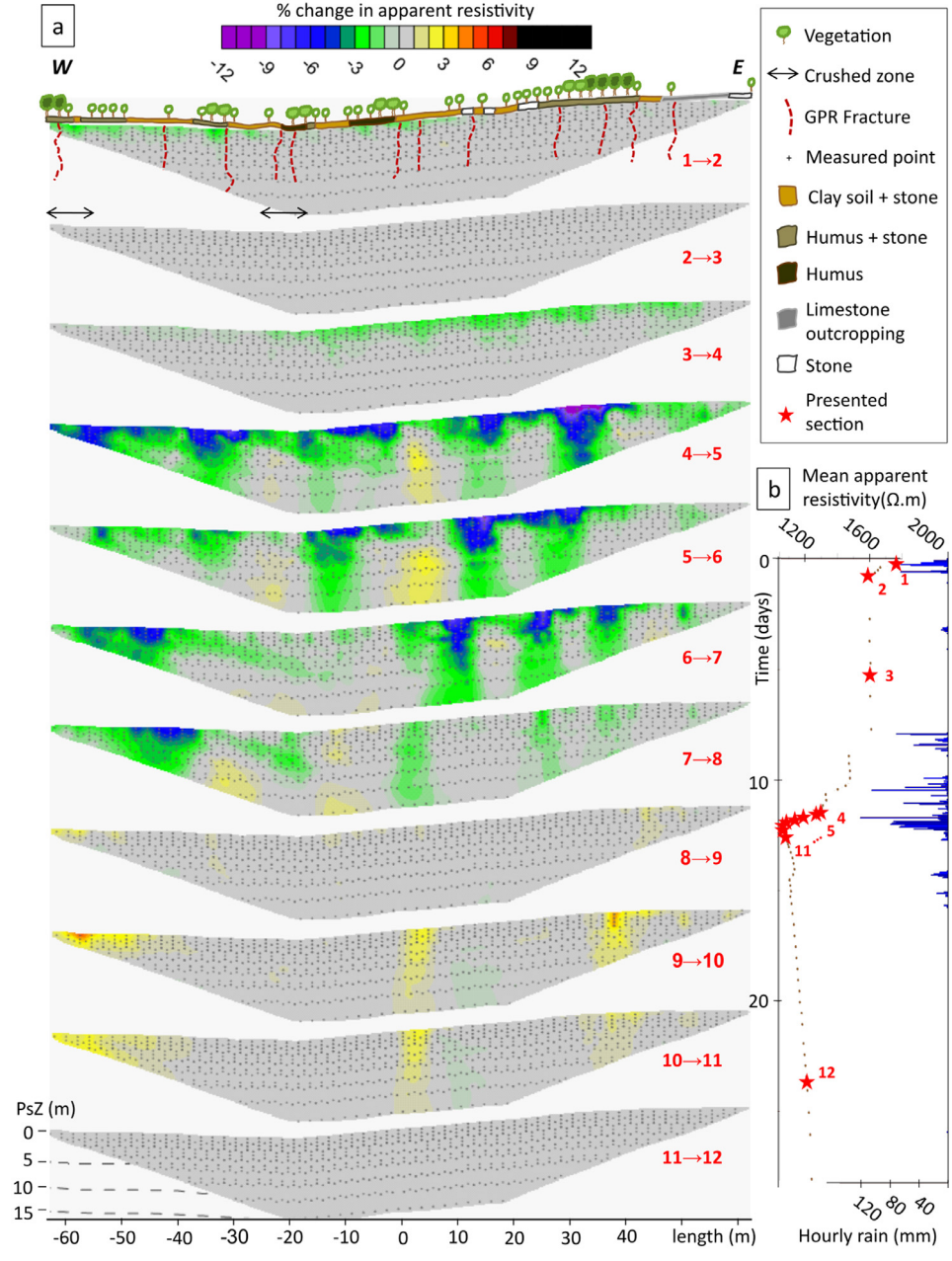

Fig. 3. (a) Hourly change in apparent resistivity between two consecutive time steps. Positioning of fracture detected by GPR and basic representation of vegetation and soil cover; (b) Evolution of mean apparent resistivity during monitoring versus rain [7]. Each brown point represents one ERT section.

identified above as preferential pathways. This second observation reinforced the hypothesis of preferential pathways playing a hydraulic role. Other zones where drainage process is not identifiable could be related with zones where soil is thicker and remains moist after the rain.

The water routes identified do not seem related with variations of vegetation density or soil cover. However, these zones seem related with fractures, faults or crushed zone previously detected by GPR [7]. Note also that the resistivity variations are different in fractures and in crushed area in the west of the profile. A crushed zone could induce a larger water route than a fracture. It is important to point out that this approach do not image the pathways but we probably image the effect of pathways above the soil.

Step 4: Data inversion is necessary to provide the electrical resistivity distribution and its evolution on the underground. Commercial and research inversion software can be applied. Several of them were tested with this dataset but results were not satisfactory [1,6]. Both simple and time-lapse inversion schemes were applied. Their results were not reflecting field evidences or even previous geological and hydrogeological findings. We assumed that the existing inversion schemes were not yet well adapted for this type of dataset.

Ethics Statement

We did not use data from human or animal subjects, nor data collected from social media platforms.

Declaration of Competing Interest

The authors declare that they have no known competing financial interests or personal relationships which have or could be perceived to have influenced the work reported in this article.

CRediT Author Statement

Simon D. Carrière: Conceptualization, Methodology, Funding acquisition, Data curation, Writing – original draft; **Konstantinos Chalikakis:** Conceptualization, Methodology, Data curation, Writing – review & editing.

Acknowledgments

The authors would like to express their gratitude to CIRAME and to all the LSBB team. The LSBB experimental site is part of the SNO H+ scientific network. The Fontaine-de-Vaucluse kast hydrosystem is part of the SNO KARST. Both SNO KARST and SNO H+ are part of the OZCAR Research Infrastructure (https://www.ozcar-ri.org/), which is supported by the French Ministry of Research, French Research Institutions and Universities. This study is founded by the French ministry of education and research for a PhD grant.

References

[1] S.D. Carrière, K. Chalikakis, C. Danquigny, R. Clément, C. Emblanch, Feasibility and limits of electrical resistivity tomography to monitor water infiltration through karst medium during a rainy event, in: B. Andreo, F. Carrasco, J.J. Durán, P. Jiménez, J.W. LaMoreaux (Eds.), Hydrogeological and Environmental Investigations in Karst Systems, Springer, Berlin Heidelberg, 2015, pp. 45–55, doi:10.1007/978-3-642-17435-3_6.

[2] T. Dahlin, B. Zhou, Multiple-gradient array measurements for multichannel 2D resistivity imaging, Near Surf. Geophys. 4 (2006) 113–123.

[3] T. Dahlin, The development of DC resistivity imaging techniques, Comput. Geosci. 27 (2001) 1019–1029, doi:10.1016/s0098-3004(00)00160-6.

[4] J.M. Puig, Le système kasrtique de la Fontaine de Vaucluse, Université d'Avignon et des Pays de Vaucluse, 1989.

[5] J.-P. Masse, M. Fenerci-Masse, Drowning discontinuities and stratigraphic correlation in platform carbonates. The late Barremian-early Aptian record of southeast France, Cretaceous Res. 32 (2011) 659–684, doi:10.1016/j.cretres.2011.04.003.
[6] S.D. Carrière, Etude hydrogéophysique de la structure et du fonctionnement de la zone non saturée du karst, Université d'Avignon et des Pays de Vaucluse, 2014.
[7] S.D. Carrière, K. Chalikakis, C. Danquigny, H. Davi, N. Mazzilli, C. Ollivier, C. Emblanch, The role of porous matrix in water flow regulation within a karst unsaturated zone: an integrated hydrogeophysical approach, Hydrogeol. J. 24 (2016) 1905–1918.